Volume 1 | Number 1 | Jan 2013 | Pages 1–100

Nanoscale

www.rsc.org/nanoscale

ROYAL SOCIETY OF CHEMISTRY

ROYAL SOCIETY OF CHEMISTRY

www.rsc.org/nanoscale

1   *Nanoscale*

2 # High-Sensitivity, Highly Transparent, Gel-Gated MoS$_2$

3 # Phototransistor on Biodegradable Nanopaper

4

5 Qing Zhang[1, 2], Wenzhong Bao[2, 3], Amy Gong[2], Tao Gong[4], Dakang Ma[4], Jiayu Wan[2], Jiaqi Dai[2],
6 Jeremy N. Munday[4], Jr-Hau He[*,3], Liangbing Hu[*,2], Daihua Zhang[*,1]

7

8 1. State Key Laboratory of Precision Measuring Technology & Instruments, College of Precision
9 Instrument and Opto-electronics Engineering, Tianjin University, Tianjin 300072, China

10 2. Department of Materials Science and Engineering, University of Maryland College Park,
11 Maryland 20742-4111, USA

12 3. Computer, Electrical and Mathematical Sciences and Engineering (CEMSE) Division, King
13 Abdullah University of Science and Technology (KAUST), Thuwal 23955-6900, Kingdom of
14 Saudi Arabia

15 4. Department of Electrical and Computer Engineering, University of Maryland, College Park,
16 Maryland 20742-4111, USA

17

18 Email: dhzhang@tju.edu.cn, binghu@umd.edu, rhau.he@kaust.edu.sa

19

20

21

22

23   **ABSTRACT:**

24   Transition metal dichalcogenides hold great promise for a variety of novel electrical, optical and

25   mechanical devices and applications. Among them, molybdenum disulphide (MoS_2) is gaining

26   increasing attention as the gate dielectric and semiconductive channel for high-perfomance field

27   effect transistors. Here we report on the first MoS_2 phototransistor built on flexible, transparent

28   and biodegradable substrate with electrolyte gate dielectric. We have carried out systematic

29   studies on its electrical and optoelectronic properties. The MoS_2 phototransistor exhibited

30   excellent photo responsivity of ~1.5 kA/W, about two times higher compared to typical back-

31   gated devices reported in previous studies. The device is highly transparent at the same time with

32   an average optical transmittance of 82%. Successful fabrication of phototransistors on flexible

33   cellulose nanopaper with excellent performance and transparency suggests that it is feasible to

34   achieve an ecofriendly, biodegradable phototransistor with great photoresponsivity, broad

35   spectral range and durable flexibility.

36

37   **KEYWORDS:** Molybdenum Disulfide phototransistor, Nanopaper substrate, Flexible

38   electronics, Biodegradable electronics, Gel-electrolyte gating

39

40

41   **Main text:**

42   Printed electronics with flexibility has attracted tremendous interests in recent years. [1-4]

43   Conventional electronics are made with a glass or plastic substrate. Glass substrates can endure

44   very high handling temperature [2] but provide poor flexibility. Plastic substrates are transparent

45   and flexible,[5] but they are not environmentally friendly and may take hundreds of years to

46   decompose. Recently, ultra-smooth transparent nanopaper with optical transmittance over 90%

47   has been developed for flexible electronics.[6-9] Nanopaper is made from the same natural wood

48   pulp material as in paper, while consisting of much thinner nanofibrillated cellulose (NFC) fibers

49   of 5 to 10 nm in diameter.[10-12] The wood fibers are treated with (2,2,6,6-tetramethylpiperidin-1-

50   yl)oxyl (TEMPO) [13, 14] to convert the hydroxyl groups to sodium carboxylate groups for

51   improved packing density.[15-18] The fibers are then disintegrated by high pressure mechanical

52   homogenizer.[9] The densely packed nanofibers leave minimal amount of air trapped in the paper

53   and give rise to very high transparency. Their ultra-small diameter also makes the paper surface

54   sufficiently smooth to be used as the supporting substrate for a variety of functional nano-

55   devices. Furthermore, the use of biodegradable natural wood pulp ensures the device is

56   environmentally friendly at the same time.[1] In a typical CMOS chip, the functional section is

57   formed by only a small portion of the chip, whereas the supporting substrate comprises more

58   than 99% of the semiconductor materials.[19] These ecofriendly transistors can help conserve non-

59   renewable natural resources by replacing toxic semiconductor materials with biodegradable

60   nanopapers.[2]

61   Phototransistor is essentially a light-sensitive field effect transistor (FET) that transduces

62   incoming photo energy to electrical current. Phototransistors based on two dimensional (2D)

63   materials have become increasingly popular in recent years.[20-22] Among them, MoS_2 has received

64   particular interest due to its unique electrical and optical properties.[23-26] In fact, devices made of

65   bulk MoS_2 have emerged decades before. [27-29] Its special band structure, mechanical flexibility

66   and ease of processing make MoS_2 an ideal candidate material for optoelectronics applications.[30]

67   Many groups have reported on MoS_2-based phototransistors fabricated on Si/SiO_2 substrates,

68   which were neither flexible nor environmental friendly.[31, 32] In this work, we demonstrate a

69   flexible, transparent and biodegradable phototransistor gated through gel-electrolyte. Two sheets

70   of nanopaper are used as the supporting substrate and the top passivation layer to sandwich the

71   MoS_2 channel and the gel-electrolyte in between. We used multilayer MoS_2 as they possess

72   higher density of states in conduction band and yield higher photo current compared to single

73   layer crystals according to theoretical predictions.[34] We have systematically characterized the

74   electrical and optoelectronic properties as well as the optical transmittance of the phototransistor.

75   The device exhibits exceptionally high photoresponsivity (~1.5 kA/W) and excellent optical

76   transmittance (~82%).
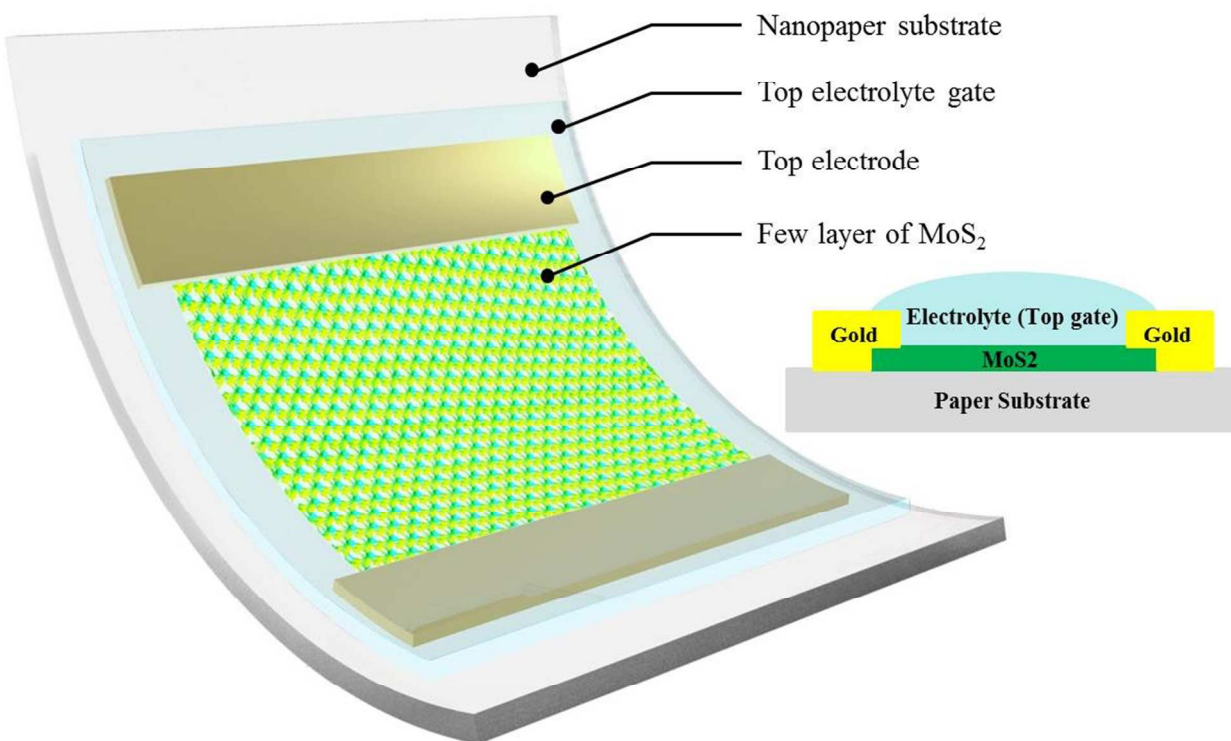
77

78   **Figure 1.** Three-dimensional schematic and cross-sectional view of the MoS_2 phototransistor on

79   transparent and flexible nanopaper (The top passivation layer is not included in this illustration).

80   Figure 1 illustrates the device structure prior to passivation. 50 nm thick gold electrodes were

81   deposited on top of a mechanically exfoliated MoS_2 flake through shadow mask. We chose

82   shadow mask over standard photolithography to avoid dissolving the nanopaper with wet

83   processes. The shadow mask also minimizes process-induced contaminations and ensures good

84   contact quality between the MoS_2 and metal electrodes. We then coated a thin layer of gel-

85   electrolyte (1 M $LiClO_4$ in w/w = 1:10[33] polyethylene oxide, see SI file) on top of the MoS_2 flake

86   as the gate dielectric[34-36] . To immobilize the gel-electrolyte and protect the active area, we

87   covered the surface with a separate sheet of nanopaper to form a conformal seal. The entire

88   process flow of the sandwich structure is summarized in Fig. 2A and in SI file.
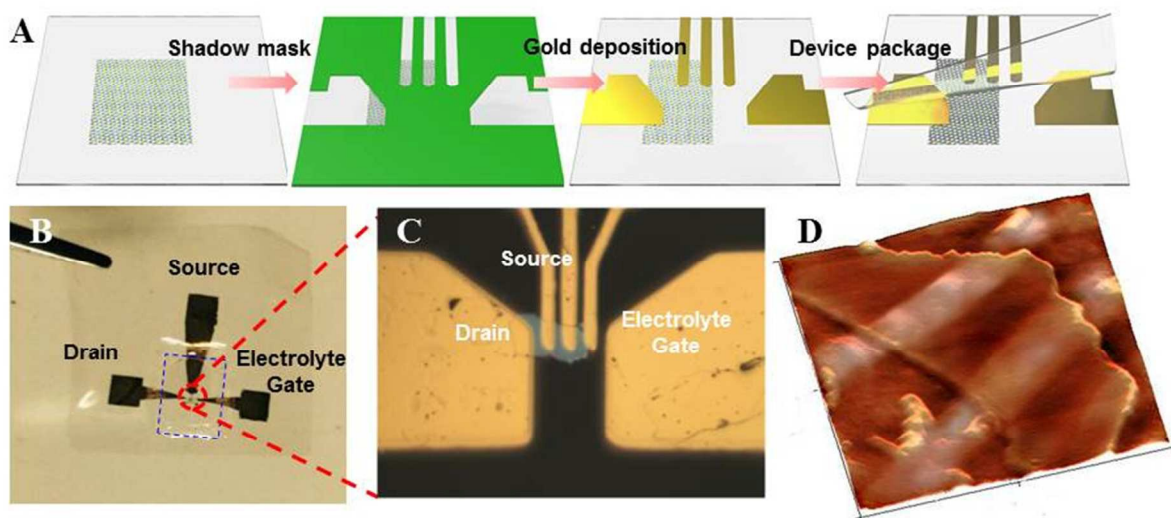
89

90   **Figure 2. A.** Fabrication process of the phototransistor. **B.** Photograph of a sealed

91   phototransistor. **C.** Optical image of zoom-in area of the phototransistor with MoS_2. **D.** An

92   atomic force microscope image of the phototransistor.

5

93   The photograph in Fig. 2B shows a sealed device. The blue dashed line identifies the edge of the

94   top sealing nanopaper. The size is large enough to cover the entire MoS_2 flake and the electrodes,

95   while small enough to expose the metal pads for probing or wire bonding. The microscope image

96   of Fig. 2C zooms into the active area of the device. The MoS_2 flake at the center serves as the

97   photo-sensitive channel. An atomic force microscopy image is shown in Fig. 2D. Thickness of

98   the MoS_2 flake was measured to be 25 nm.
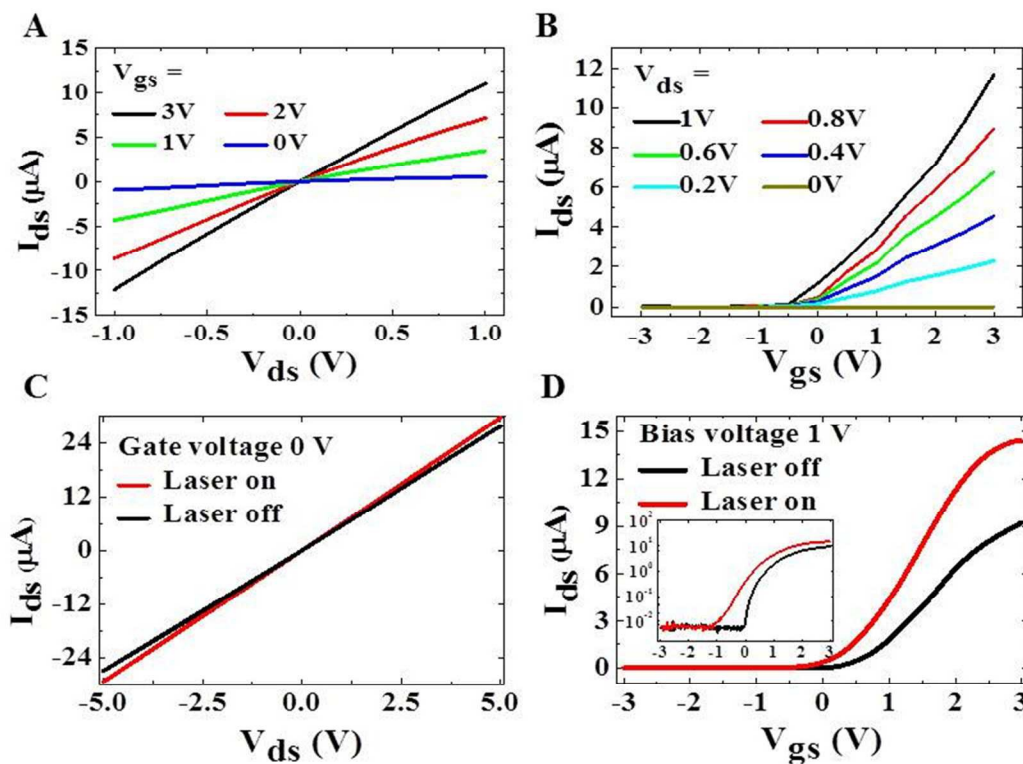
99

100   **Figure 3. Room temperature electrical and optoelectrical properties of the MoS_2**

101   **phototransistor. A.** Output ($I_{ds}-V_{ds}$) characteristics of the phototransistor under different gate

102   voltages. **B.** Room temperature transfer characteristics ($I_{ds}-V_{gs}$) of the same phototransistor at

103   different source-drain biases. **C.** $I_{ds}-V_{ds}$ at V_{gs} = 0V before (black) and after (red) exposure to

104   laser illumination. The power of the incident laser is 15 μW, and the wavelength is 532 nm. **D.**

105   Transfer characteristics ($I_{ds} - V_{gs}$) before (black) and after (red) exposure to laser. The inset shows

106   the same data in log scale.

107   The electron transport properties of the phototransistor are characterized at room temperature in

108   atmosphere. Before the characterization, we took an I-V measurement on a blank nanopaper and

109   estimated the leakage current to be < 2pA under 5V (SI file). Fig. 3A shows the $I_{ds} - V_{ds}$ curves

110   under four different gate biases, which are linear and symmetric, indicating good contact quality

111   between the MoS_2 channel and Au electrodes. The lithography-free fabrication eliminates the

112   need of adhesion metals and prevents contaminations associated with wet processes, resulting in

113   highly stable conductance and superior carrier mobility compared to previous work (see SI

114   file).[Error! Bookmark not defined., 37]

115   The transfer curves ($I_{ds} - V_{gs}$) of the MoS_2 phototransistor are presented in Fig. 3B, revealing a

116   typical n-type semiconducting behavior, which is consistent with previous reports.[4, 6, 8, 9] Fig. 3C

117   shows the $I_{ds} - V_{ds}$ curves of the phototransistor when illumination is on (red) and off (black),

118   respectively. Under stable and continuous illumination (532 nm, 15μW), the incident laser can

119   generate a significant photocurrent in the phototransistor. We compare the transfer characteristics

120   with (red curve) and without (black curve) the illumination in Fig. 3D. In the dark state, the

121   phototransistor shows a threshold voltage of $V_t = 0.4$ V, which shifts to $V_t = 0.1$ V when the

122   illumination is on. .

123
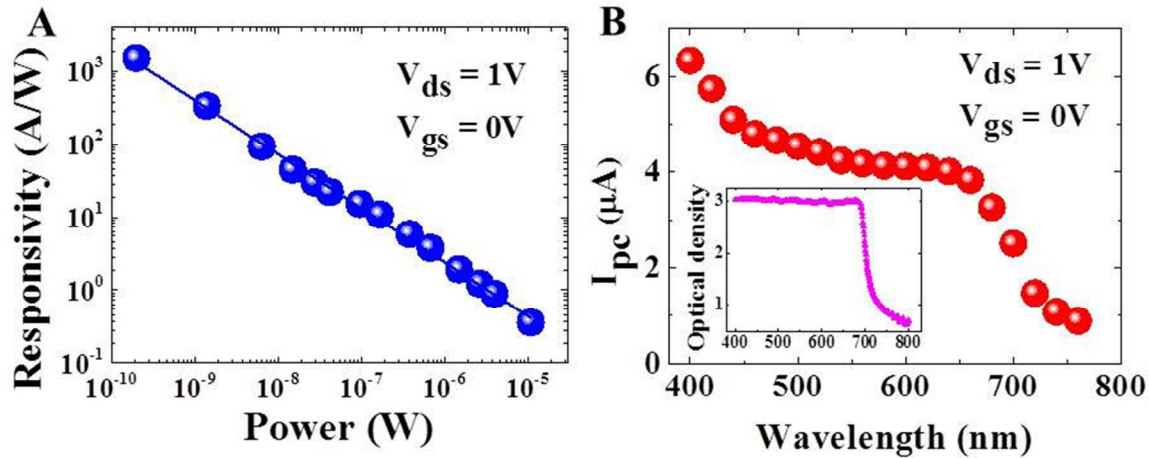
Figure 4. Photo response of the MoS$_2$ phototransistor. A. Photoresponsivity of the device as a function of illumination power. The fitting uses $\sim E^{\beta-1}$, where E is the illumination power; β is the constant **B.** Photocurrent of the same MoS$_2$ device at different wavelengths under V_{ds} = 1 V and V_{gs} = 0 V. The inset shows the absorption curve of the MoS$_2$.

We further explored the photo detection performance of the device, characterized by its external photoresponsivity R, defined as the ratio of the photocurrent (I_{pc}) and the incident illumination power (P_{in}):

$$R = \frac{I_{pc}}{P_{in}}$$

As shown in Fig. 4A, the responsivity decreases with increasing illumination power (E), which is consistent with the observation in previous studies.**Error! Bookmark not defined.** A quantitative correlation between R and E can be written[38] as:

$$R \sim E^{\beta-1}$$

The equation has been successfully applied to other phototransistors based on single-layer MoS$_2$,

135   graphene and PbS.[37] By fitting the data (in SI file), we derived to be 0.26. The parameter reflects

136   the recombination dynamics of photo induced carriers [39] and ranges between 0.2 to 0.7 in

137   previous studies.[39, 40] The decrease in responsivity with incident optical power is commonly

138   observed in phototransistors according to other reports.[20, **Error! Bookmark not defined.**, 41] This effect is

139   presumably associated with a reduction of the number of photo generated carriers available for

140   extraction under high photon flux due to Auger processes or the saturation of recombination and

141   trap states that influence the lifetime of the generated carriers.[39] In addition, we note that the

142   responsivity of our device is considerably higher than the average value reported in literatures.

143   The maximum value reached 1.5 kA/W at 10nW illumination power (see SI file for more

144   information), while the highest responsivity measured with back gated MoS_2 phototransistors are

145   typically below 1kA/W.[26,30] We believe both the lithography-free fabrication and the electrolyte

146   gating contribute to the responsivity enhancement, and the latter plays a more dominant role. The

147   electrolyte we used is a liquidized salt that contains cations (Li^+).[33] The cations accumulate on

148   MoS_2 surface under an externally applied voltage, forming an electric double layer (EDL). The

149   EDL is able to effectively screen charge impurities and reduce electron scattering, thereby

150   largely boosting the carrier mobility by 1 to 2 orders of magnitude.[42] At the same time, the

151   electrolyte can also induce strong band bending at the MoS_2/Au interface and significantly lower

152   the Schottky barrier.[43, 44] The large enhancement in both intrinsic and extrinsic mobility is

153   presumably the reason for the exceedingly high responsivity observed in our phototransistors.

154   We have also measured the dark/light current across a wide range of wavelengths (Fig. 4B).

155   When the incident laser is above 685 nm, the photocurrent drops sharply with increasing

156   wavelength. The transition around 685 nm corresponds to the excitation of electrons across the

157   bandgap (1.81eV) of multilayer MoS_2. The same transition is also evidenced in the absorption

158   curve in the inset. Below 685 nm, the slow and monotonic increase in photocurrent with

159   decreasing wavelength (or increasing photon energy) is presumably due to the fact that higher

160   energy photons can excite electrons to higher energy states, resulting in a larger number of

161   photocarriers that can overcome local energy barriers in the conduction channel and/or at the

162   MoS_2/metal interface.
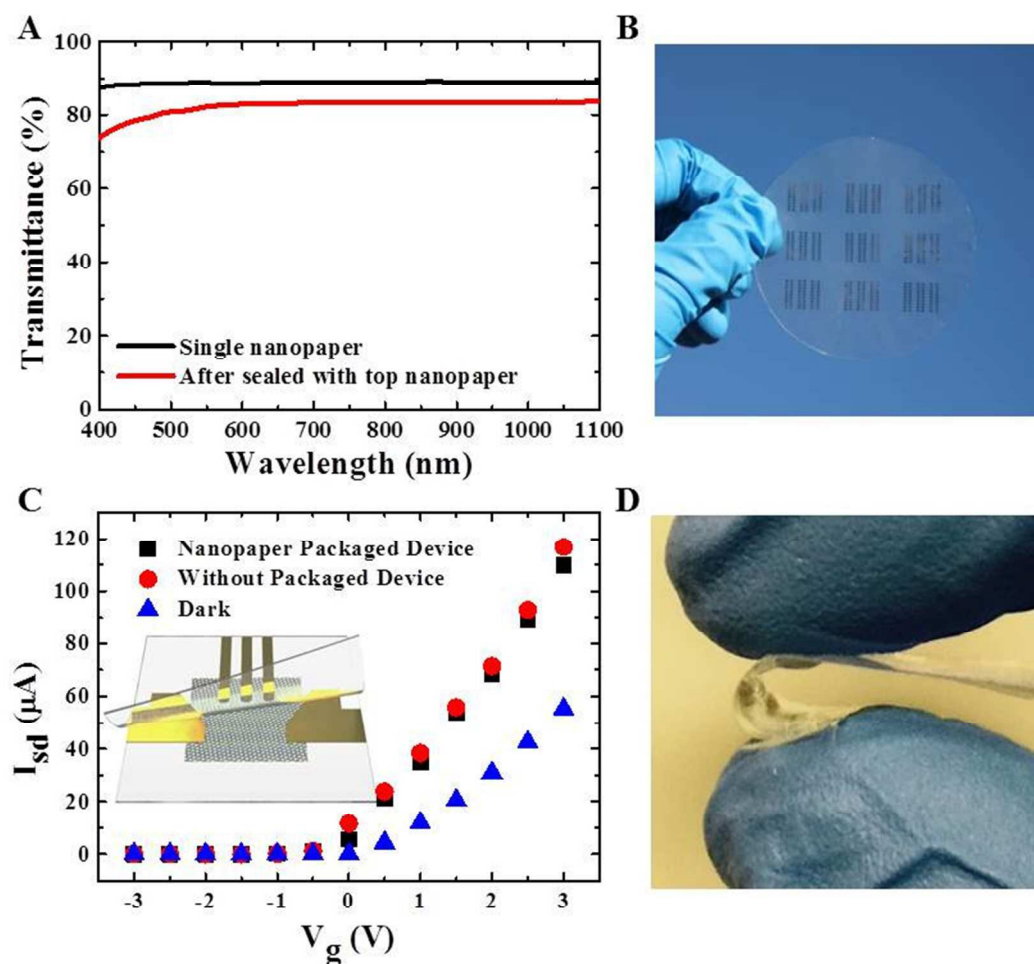
163

164   **Figure 5. Optical transmittance, transparency and flexibility of the MoS_2 phototransistor.**

165   **A.** Optical transmittance of a single sheet of nanopaper (black line) and a MoS_2 phototransistor

166   sandwiched between two layers of nanopaper (red line). **B.** Photograph of an array of

167   phototransistors showing high transparency. **C.** Transfer characteristics of the phototransistor

168   without illumination (blue), under illumination but without passivation (red), and with both

169   illumination and passivation (black). **D.** The device can be largely bended, exhibiting great

170   flexibility.

171   Besides excellent photoresponsivity, the phototransistor is highly transparent and flexible at the

172   same time. In Fig. 5A, we compare the optical transmittance of the device (red curve) with a

173   sheet of bare nanopaper (black curve) across a broad spectral range from 400 nm to 1100 nm.

174   When compared at 550 nm, the optical transmittance of the phototransistor (82%) is slightly

175   lower than that of the bare nanopaper (85%) due to the addition of gel-electrolyte and passivation

176   layer. Fig. 5B and 5D demonstrate the excellent flexibility of the device and its compatibility

177   with large-scale integration. The electrical and photodetection properties remain nearly the same

178   before and after bending (in SI file). To verify that the passivation layer induces negligible

179   perturbation to the phototransistor, we have recorded the transfer curves before and after

180   passivation (Fig. 5C). In the dark state, the two devices behave the same as indicated by the data

181   points in blue triangle. Under illumination (532 nm), the bare device shows slightly higher

182   current compared at the same gate bias. The difference at V_{gs} = 3 V is approximately 6 µA

183   between the two devices. The result is in good agreement with the optical transmittance response

184   in Fig. 5A, in which the sealed phototransistor has a slightly lower optical transmittance

185   therefore less sensitive to the incident laser.

186   **Summary**

187   We have demonstrated an electrolyte gated phototransistor based on multilayer MoS_2. The device

188   uses highly transparent, flexible and biodegradable nanopaper as both the supporting substrate

189   and passivation layer. It exhibits excellent photoresponsivity of approximately 1.5 kA/W under

190   10nW illumination power, considerably higher than typical back gated phototransistors reported

191   in other studies. The device functions across a broad spectral range with excellent stability under

192   sustained voltage bias and illumination. These properties make the device highly attractive for

193   various industrial applications including touch sensor panels, image sensors, solar cells, and

194   intelligent displays.

195

196   **EXPERIMENTAL SECTION**

197   **Fabrication of Transparent Nanopaper.**   The nanopaper was fabricated by previously

198   established method published by Zhu. et al.[8] The experimental procedure includes three major

199   steps: (2,2,6,6-tetramethylpiperidin-1-yl)oxyl (TEMPO) oxidation reaction, Büchner filtration,

200   and disintegration through a microfluidizer (M110 EH, Microfluidics Inc., USA). TEMPO-

201   mediated oxidation started by adding and dissolving 78 mg TEMPO into 25 mL buffer solution.

202   The buffer consists of 0.08 M Sodium carbonate (Na_2CO_3), and 0.02 M Sodium bicarbonate

203   ($NaHCO_3$). Combine three solutions, that is, 78 mg TEMPO in 25 mL buffer, 514 mg of sodium

204   bromide (NaBr) in 50 mL buffer and 5 g dry weight of Kraft bleached softwood pulp in 115 mL

205   buffer solution. The solution was stirred at a speed of 700 rpm with IKA RW20 digital mixer for

206   10 min followed by drop-wise addition of 35 mL sodium hypochlorite (NaClO). The pH value

207   of the solution was measured every 20 mins and kept at pH=10.5 by adding 3M sodium

208   hydroxide (NaOH) for 2 hours. Reaction with continuous stirring 700 rpm lasted overnight at

209   room temperature. Then, the TEMPO-oxidized fibers were transferred to a vacuumed flask and

210   funnel for Büchner filtration using 0.65 μm nitrocellulose ester filter (Millipore DAWP29325) to

211   wash away the reagents. Fiber was washed by 1L deionized (DI) water by stirring at 800 rpm for

212   30 min and passing through Büchner funnel into a flask twice. The resulting fiber cake was

213   dissolved in DI water to form a 1 wt% solution and passed through a microfluidizer with thin z-

214   shaped chambers. The channel dimension was 200 μm and the process pressure was 25,000 psi.

215   After passing through the microfluidizer the fibers were dispersed in water to create a 1 wt%

216   nanofibrillated cellulose (NFC) solution. The NFC solution was further diluted with DI water to

217   0.2 wt% and mixed at 500 rpm for 10 min with IKA RW20 digital mixer. After that, the

218   dispersion was degassed in a bath sonicator for 20 min, and passed through a 0.65 μm pore size

219   nitrocellulose eater filter (Millipore DAWP29325). The cake formed was compressed between a

220   PET film (on top) and papers supported by iron plate (below). Then, it was transferred to a hot

221   pressing machine in 105 ℃ for 4-5 days to form nanopaper with a fiber diameter of about 5 nm.

222

223   **Reference:**

1 Y. H. Jung, T. -H. Chang, H. Zhang, C. Yao, Q. Zheng, V. W. Yang, H. Mi, M. Kim, S. J. Cho, D. -W. Park, H. Jiang, J. Lee, Y. Qiu, W. Zhou, Z. Cai, S. Gong and Z. Ma, *Nat. Commun.*, 2015, **6**: 7170.

2 J. Huang, H. Zhu, Y. Chen, C. Preston, K. Rohrbach, J. Cumings and L. Hu, *ACS Nano*, 2013, **7**: 2106-2113.

3 A. Kulachenko, T. Denoyelle, S. Galland and S. B. Lindstrom, *Cellulose*, 2012, **19**, 793-807.

4 H. Zhu, Z. Xiao, D. Liu, Y. Li, N. J. Weadock, Z. Fang, J. Huang and L. Hu, *Energy & Environmental Science*, 2013, **6**, 2105-2111.

5 W. A. MacDonald, M. K. Looney, D. MacKerron, R. Eveson, R. Adam, K. Hashimoto and K. Rakos, *Journal of the Society for Information Display*, 2007, **15**, 1075-1083.

6 D. O. Carlsson, G. Nystrom, Q. Zhou, L. A. Berglund, L. Nyholm and M. Stromme, *Journal of Materials Chemistry*, 2012, **22**, 19014-19024.

7 Z. Fang, H. Zhu, Y. Yuan, D. Ha, S. Zhu, C. Preston, Q. Chen, Y. Li, X. Han, S. Lee, G. Chen, T. Li, J. Munday, J. Huang and L. Hu, *Nano Lett.*, 2014, **14**, 765-773.

8 H. Zhu, S. Parvinian, C. Preston, O. Vaaland, Z. Ruan and L. Hu, *Nanoscale*, 2013, **5**, 3787-3792.

9 I. Siro, D. Plackett, M. Hedenqvist, M. Ankerfors and T. Lindstrom, *Journal of Applied Polymer Science*, 2011, **119**, 2652-2660.

10 H. Zhu, Z. Fang, C. Preston, Y. Li and L. Hu, *Energy & Environmental Science*, 2014, **7**, 269-287.

11 M. Nogi, C. Kim, T. Sugahara, T. Inui, T. Takahashi and K. Suganuma, *Appl. Phys. Lett.*, 2013, **102**, 181911.

12 M, Nogi, S. Iwamoto, A. N. Nakagaito and H. Yano, *Adv. Mater.*, 2009, **21**, 1595-1598.

13 T. Saito and A. Isogai, *Biomacromolecules*, 2004, **5**, 1983-1989.

14 T. Saito, Y. Okita, T. T. Nge, J. Sugiyama and A. Isogai, *Carbohydrate Polymers*, 2006, **65**, 435-440.

15 A. Isogai and Y. Kato, *Cellulose*, 1998, **5**, 153-164.

16 D. Klemm, F. Kramer, S. Moritz, T. Lindstrom, M. Ankerfors, D. Gray and A. Dorris, *Angewandte Chemie-International Edition*, 2011, **50**, 5438-5466.

17 R. T. Olsson, M. A. S. A. Samir, G. Salazar-Alvarez, L. Belova, V. Strom, L. A. Berglund, O. Ikkala, J. Nogues and U. W. Gedde, *Nat. Nanotech.*, 2010, **5**, 584-588.

18 H. Fukuzumi, T. Saito, T. Wata, Y. Kumamoto and A. Isogai, *Biomacromolecules*, 2009, **10**, 162-165.

19 J.P. Colinge, *Silicon-on-Insulator Technology: Materials to VLSI 3rd edn., Ch.1*, Springer 2004.

20 Z. Y. Yin, H. Li, H. Li, L. Jiang, Y. M. Shi, Y. H. Sun, G. Lu, Q. Zhang, X. D. Chen and H. Zhang, *ACS nano*, 2012, **6**, 74-80.

21 W. G. Luo, Y. F. Cao, P. G. Hu, K. M. Cai, Q. Feng, F. G. Yan, T. F. Yan, X. H. Zhang and K. Y. Wang, *Adv. Opt. Mater.*, 2015, **3**, 1418-1423.

22 S. C. Dhanabalan, J. S. Ponraj, Q. Bao and H. Zhang, *Nanoscale*, 2016.

23 H. Zhang, *ACS Nano*, 2015, **9(10)**:9451-9469.

24 H. Li, J. Wu, Z. Yin, H. Zhang, *Acc. Chem. Res.*, 2014, **47(4)**: 1067-1075.

25 X. Huang, Z. Zeng, H. Zhang, *Chem. Soc. Rev.*, 2013, **42(16)**: 1934-1946.

26 W. Zhang, J. K. Huang, C. H. Chen, Y. H. Chang, Y. J. Cheng and L. J. Li, *Adv. Mater.*, 2013, **25(25)**, 3456-3461.

27 W. Choi, M. Y. Choi, A. Konar, J. H. Lee, G. B. Cha, C. H. Soon, S. Kim, J. Kim, D. Jena, J. Joo and S. Kim, *Adv. Mater.*, 2012, **24(43)**, 5832-5836.

28 P. Joensen, R. F. Frindt and S. R. Morrison, *Mater. Res. Bull.*, 1986, **21**, 457-461.

29 D. B. Velusamy, R. H. Kim, S. Cha, J. Huh, R. Khazaeinezhad, S. H. Kassani, G. Song, S. M. Cho, S. H. Cho, I. Hwang, J. Lee, K. Oh, H. Choi and C. Park, *Nat. Commun.*, 2015, **6**: 8063

30 F. H. L. Koppens, T. Mueller, Ph. Avouris, A. C. Ferrari, M. S. Vitiello and M. Polini, *Nat. Nanotech.*, 2014, **9**, 780-793.

31 S. Kim, A. Konar, W. S. Hwang, J. H. Lee, J. Lee, J. Yang, C. Jung, H. Kim, J. B. Yoo, J. Y.; Choi, Y. W. Jin, S. Y. Lee, D. Jena, W. Choi and K. Kim, *Nat. Commun.*, 2012, **3**: 1011.

32 Q. H. Wang, K. K. Zadeh, A. Kis, J. N. Coleman and M. S. Strano, *Nat. Nanotech.*, 2012, **7**, 669-712.

33 X. Cai, A. B. Sushkov, M. M. Jadidi, L. O. Nyakiti, R. L. Myers-Ward, D. K. Gaskill, T. E. Murphy, M. S. Fuhrer, and H. D. Drew, *Nano Lett.*, 2015, **15**, 4295−4302

34 Y. J. Zhang, J. T. Ye, Y. Yomogida, T. Takenobu, and Y. Iwasa, *Nano Lett.*, 2013, **13**, 3023.

35 Lhuillier, E., Robin, A., Ithurria, S., Aubin, H. and Dubertret, B., *Nano Lett.*, 2014, **14**, 2715–2719

36 Froehlicher, G. & Berciaud, S., *Phys. Rev. B*, 2015, **91**, 205413.

37 J. Kwon, K. Y. Hong, G. Han, I. Omkaram, W. Choi, S. Kim and Y. Yoon, *Adv. Mater.*, 2015, **1**, 2224-2230.

38 Zhenhua Sun, Zhike Liu, Jinhua Li, Guoan Tai, Shu-Ping Lau and Feng Yan, *Adv. Mater.*, 2012, **24**, 5878–5883.

39 M. Buscema, D. J. Groenendijk, S. I. Blanter, G. A. Steele, H. S. Zant and A. Castellanos-Gomez, *Nano Lett.*, 2014, **14**, 3347-3352.

40 H. Xu, J. Wu, Q. Feng, N. Mao, C. Wang and J. Zhang, *Small*, 2014, **10**, 2300-2306.

41 H. S. Lee, S.-W. Min, Y.-G. Chang, M. K. Park, T. Nam, H. Kim, J. H. Kim, S. Ryu and S. Im, *Nano Lett.*, 2012, **12**, 3695-3700.

42 F. Wang, P. Stepanov, M. Gray, C. N. Lau, M. E. Itkis and R. C. Haddon, Nano Lett., 2015, **15**, 5284 5288.

43 M. M. Perera, M.-W. Lin, H.-J. Chuang, B. P. Chamlagain, C. Wang, X. Tan, M. M.-C. Cheng, D. Toma´nek and Z. Zhou, ACS nano 2013, **7(5)**: 4449-4458.

44 I. Popov, G. Seifert and D. Tomanek, Physical Review Letters, 2012, 108, 156802.